SREENIVASA RAO ISLAVATH
and
DEBASIS DEB

Support design for the underground metal mine using numerical modelling techniques

A virgin chromite orebody located in eastern India is planned to be extracted by sub-level open stoping method. The portal of the decline and vertical shaft is planned to locate in the footwall side of the orebody to access the deposit. Design of proper supporting system for the underground stope is important for the safe extraction of orebody. In this paper, two dimensional finite element modelling techniques have been employed to determine the stress and displacement distributions around the stope and rib pillar and also estimated the tensile zone that may occur in the crown, sill and rib pillars. Based on development of the stress, displacement and tensile zone in the roof and rib pillar; roof bolting grid pattern is established.

Keywords: Finite element model, rib pillars, stope, joints, principal stress and bolt.

1. Introduction

Out of total reserves in India, 95% of chromite occurs in Odisha, and it has wide usage in chemical and metallurgical industries [1-3]. The chromite deposit in study extends 290m in strike length with an average width of 20m. The top portion of the deposit is located about 30m below the surface and extends vertically up to 200m. The dip angle of the orebody is 100 degree with the horizontal or 800 degree with the vertical. Country rocks of chromite deposit are weathered serpentinite, serpentinite, quartzite and pyroxenite. A quartzite hill exists on the surface towards the dip side of the orebody. The bottom most RL of the surface is 210 mRL [2].

It is proposed that the chromite orebody will be extracted by sub-level open stoping method with late filling, if required. For this purpose, a vertical circular shaft and a decline need to be developed to access the orebody. The shaft will be located in the footwall side of the orebody. The portal of the decline will also be located in the footwall side of the orebody. The top most cross-cut from the decline will contact the orebody at 170 mRL. This study is required to be conducted to determine suitable supporting system for the proposed stoping operation. In order to perform such tasks, borehole rock samples have been tested to estimate the engineering parameters of the country rocks and orebody. Rock mass rating (RMR) and geological strength index (GSI) have also been estimated for the same. Two dimensional numerical modelling techniques have been employed to estimate the stress and displacement distributions in the crown, sill and rib pillars and walls of the stopes [2-3].

Mr. Sreenivasa Rao Islavath, Assistant Professor, Department of Mining Engineering, University of Engineering (KU), Kothagudem 507 101. E-mail: islavathsreenivas@gmail.com and Dr. Debasis Deb, Professor, Department of Mining Engineering, IIT Kharagpur 721 302. E-mail: deb.kgp@gmail.com

2. Material properties of the country rock and orebody

The rock core samples of country rock and orebody collected from the mine site were prepared to the size recommended by the International Society of Rock Mechanics (ISRM) [4-5]. The length to diameter ratio of the uni-axial compressive strength and the tensile strength are 2.5 to 3.0 and 0.5 respectively. The UCS, tensile strength, modulus of elasticity, density and Poisson's ratio of the rock samples are determined in the laboratory to use as input to the numerical model and are listed in Tables 1 and 2.

TABLE 1: MATERIAL PROPERTIES OF COUNTRY ROCK AND OREBODY

Rock type	W.serpentinite	Serpentinite	Chromite	Pyroxenite	Quartzite
UCS (MPa)	132	152.56	113.18	115	110
σ_t (MPa)	4.05	11.82	10.33	3.2	3.5
ρ (kg/m^3)	2745	2745	3537.9	2350	3000

3. Numerical modelling for the support design of proposed method

3.1 THE FINITE ELEMENT METHOD

Finite element method is an effective tool for the analysis of mechanical and structural components of machinery. This method is amenable to systematic computer programming and offers a scope for application to a wide range of problems for analysis. This method is now adopted in almost all branches of engineering where complex structures, fluid dynamics problems, mine and tunnel structures and similar problems are addressed [6-8].

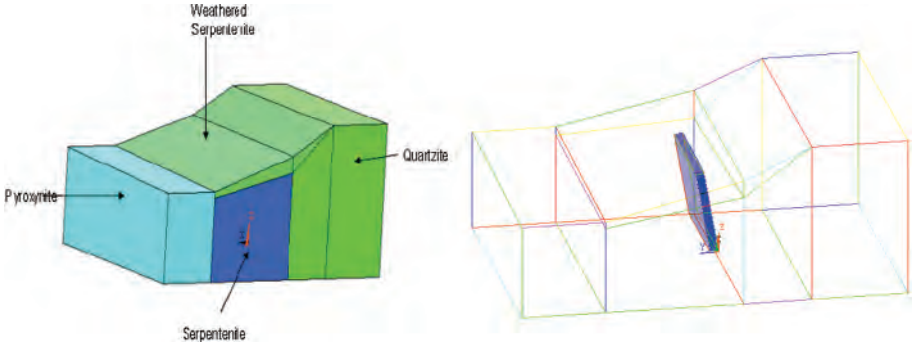

(a) Solid model showing the country rock (b) Line diagram showing the orebody

Fig.1 Model of the study area

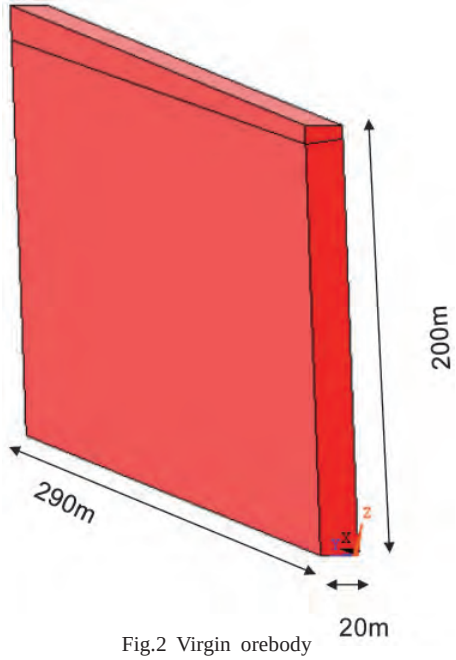

Fig.2 Virgin orebody

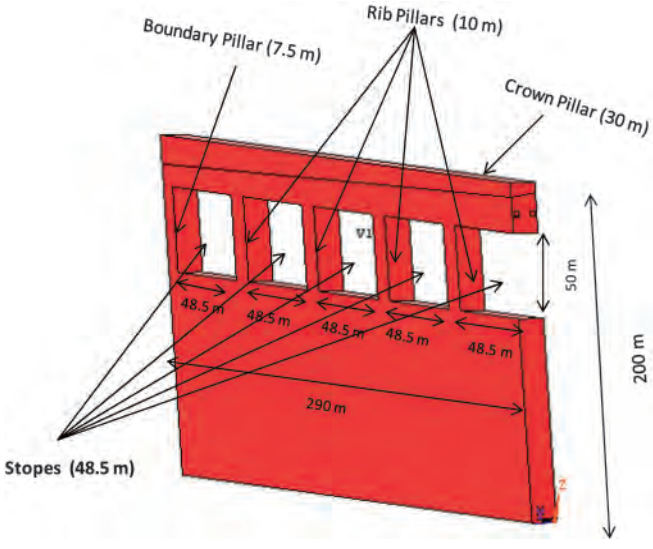

Fig.3 Developed orebody

The basic concept in this approach is that a body or structure can be divided into a finite number of smaller units of finite dimensions called ‘elements’. The original body or structure is then considered as an assemblage of these elements connected at finite number of joints called 'nodes' or ‘nodal points’. The properties of these elements are formulated and combined to obtain the solution for the entire body or structure. The global system of equations is developed as follows [7].

$$\{F\} = [K]\{q\} \quad \text{... (1)}$$

where,

{F} = global force vector, i.e. forces in each node,

[K] = global stiffness matrix based on material properties,

{q} = displacement vector containing each node.

Necessary (essential) boundary conditions in terms of displacements at some selected nodes are applied before solving this system of equations.

3.2 Two dimensional finite element model

2D-finite element models have been developed to analyze the stress and displacement distribution around the stope and the rib pillar and also have been estimated the plastic zone around the stope and rib pillars. The primary motivation of analyzing in 2D is to determine the failure zone in the roof of the stope. All 2D models are analysed considering Drucker-Prager materials in plane strain conditions [2-3]. In order to do the above task, longititudinal section of the three dimensional model (Fig.1) along the strike length of orebody is considered. This section comprises host rock (weathered serpentenite and serpentenite), orebody, stope and the rib pillars are shown in Fig.4.

The excavation model of longititudinal section consists of stope and rip pillars and surrounding rock (Fig.4a). Five stopes have been developed of 48.5m in length and 20m in width considering 50m of level interval. Four rib pillars of width 10m each are left in between the two adjacent stopes (Fig.4a). Fig.4b shows the in-situ model consists of insitu orebody and the host rock (weathered serpentenite and serpentenite) [2].

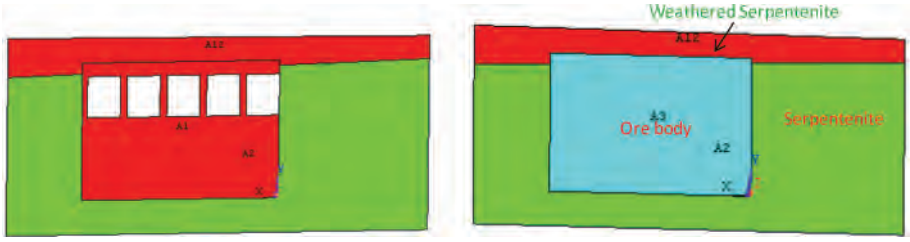

(a) Excavation model (b) Insitu model

Fig.4 Longititudinal section

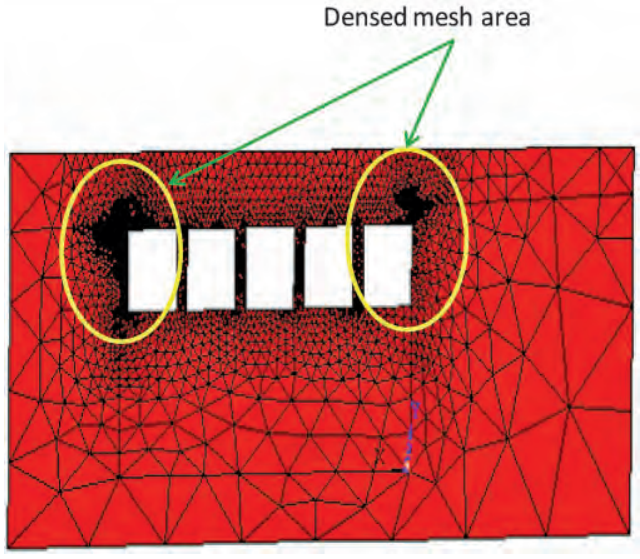

Fig.5 Finite element mesh model

3.2 Rock mass properties

Rock mass properties of country rock and orebody have been further reduced to simulate more jointed rock mass conditions. Table 2 lists the rock mass properties are used for finite element modelling for all 2D models. It can be easily seen that compressive strength of rock mass of each rock type is considered at the lower side to incorporate jointed rock mass with few centimetre spacing, weathered and watery conditions [2].

3.3 Finite element meshed models

The meshing of the excavation model produced an average of around 4,175 6-noded triangular elements and around 8,715 nodes (Fig.5). Little variations are noted in node counts with in-situ model geometries. As before, finer mesh is developed around the stope area. In those zones, finer mesh is required for better evaluation of displacements, stresses and strains. Coarse mesh is developed in the rock-body away from the mining-affected zones (zone of no-rock movement due to mining) [2].

3.4 Loading and boundary conditions

Both in situ and excavation models are constrained from two sides, those are (i) perpendicular to the strike of orebody (ii) bottom surface. Surface traction pressure is applied to another side as shown in Fig.6. Gravity loading is assumed for vertical direction. The following equation is used for calculation of horizontal stress in finite element model according to depth of the orebody [2].

$$\sigma_H = \sigma_v \quad \ldots \quad (2)$$

where, σ_H is horizontal stress along the strike of the orebody and is σ_v vertical stress.

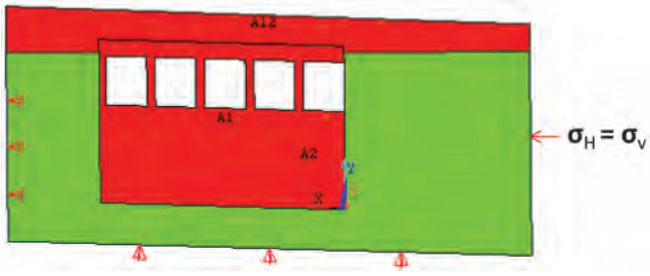

Fig.6 Boundary conditions

4. Results and discussions

All 2D finite element models have been analyzed using elasto-plastic behaviour of rock materials in plain strain condition. Results are enumerated in terms of principal stress and plastic strains distributions around the excavations [2].

4.1 Major principal stress (σ_1) distribution

The major principal stress distribution around the stope is shown in Fig.7. It is found that high stress concentration occurs at the corners of the stope. The peak major principal stress may range in between 3.43 MPa and 31.8 MPa.

Table 2: Rock mass properties used in the models

Rock strata	Modulus of elasticity (GPa)	Poisson's ratio (v)	Density ρ (kg/m^3)	Cohesion (MPa)	Friction angle (deg)	Flow angle (deg)
Weathered serpentinite	1.84	0.138	2745.0	3.00	35	17.5
Serpentinite	4.064	0.138	2745.0	1.25	25	12.5
Chromite	6.816	0.144	3537.9	1.25	20	10
Quartzite	5.090	0.150	2350.0	4.00	40	20
Pyroxenite	1.718	0.200	3000.0	4.18	20	10

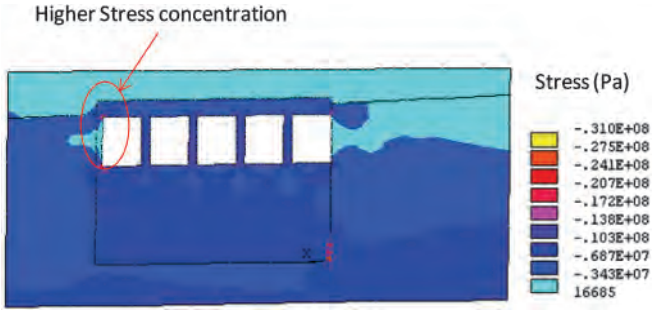

Fig.7 Major principal stresses of vertical section

4.2 Minor principal stress (σ_3) distribution

Distribution of minor principal stresses around the area is plotted in Fig.8. Tensile stress develops in the crown pillar and rib pillar. Tensile stress ranges in between leass than 1.0 MPa and 2.0 MPa depending on the location. As also found in 3D model, the developed tensile stress may cause plastic strains (yield zone) around the excavation. It is also observed that tensile zone may extend up to 2 m inside the crown pillar.

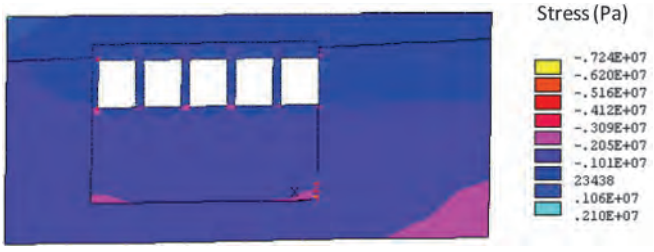

Fig.8 Minor principal stresses of vertical section

4.3 Plastic zone

As mentioned earlier, the 2D vertical section has been analyzed to determine the plastic zone in the rock mass surrounding the decline. Fig.9 shows the intensity of plastic strains that has developed around the stope area. The intensity of plastic strain varies between 0 and 0.002343. These results clearly signify that proper support system is required to protect the crown and rib pillar and the stope walls. The results also show that a corner of the crown pillar may yield due to concentration of shear stress.

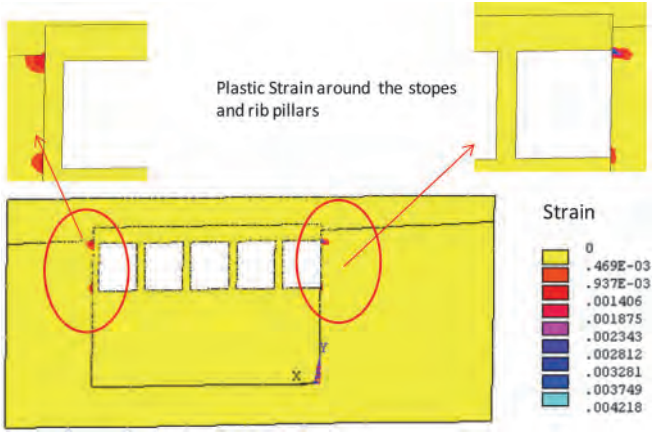

Fig.9 Distribution of intensity of plastic strain

4.4 Design of rock bolt

As mentioned before, hanging wall and part of footwall will need support to reduce tensile stress. Fully grouted rock bolts are considered to be one of the most cost-effective and efficient primary rock reinforcing tools. In the following the spacing of rock bolts is determined for 2.4 m rock bolts having steel of tensile strength of 500 MPa [2].

Assuming a square spacing of meter, the rock load and support load of the bolt can be equated for 60% of its strength as given below [7, 9].

$$S^2 \times L \times \gamma_r = 0.6 \times \sigma_y \times \frac{\pi d^2}{4} \quad \ldots \quad (3a)$$

$$S = \sqrt{\frac{0.6 \times \sigma_y \times \pi d^2}{4 \times L \times \gamma_r}} \quad \ldots \quad (3b)$$

where, S is spacing between the two adjacent holes (m); σ_y is yield strength of bolt steel (MPa); d is diameter of the rock bolt (m); L is length of the rock bolt (m) and $\gamma_r = \rho \times g$ is specific unit weight of rock (kN/m^3).

For determining the spacing (S) between the two adjacent holes, the length of the bolt, diameter of the bolt and yield sterght of the bolt are 2.4 m, 22 mm and 500 MPa respectively. Based on equation 3, spacing between two adjacent holes is estimated as given below.

$$S = \sqrt{\frac{0.6 \times 500 \times 10^6 \times \pi \times 0.022^2}{4 \times 2.4 \times 34.7 \times 10^3}} = 1.17 \text{ m} = 1.2 \text{ m}$$

(approximately).

Hence, a maximum spacing of 1.2 m is required for rock bolts having length of 2.4 m, diameter of 22 mm and yield strength of 500 MPa.

4.5 Joint analysis

As described above, longititudinal section of the study area has been taken along the strike of orebody to do the detail joint analysis. Fig.10 shows the location for the joint analysis in the rib pillar and the set of joints in the rib pillar [2].

The major (σ_1) and minor (σ_3) principal stresses are estimated as follows [7, 9].

$$\sigma_1 = \left(\frac{\sigma_{xx} + \sigma_{yy}}{2}\right) - \left\{\left(\frac{\sigma_{xx} - \sigma_{yy}}{2}\right)^2 + \tau_{xy}^2\right\}^{1/2} \quad \ldots \quad (4a)$$

$$\sigma_3 = \left(\frac{\sigma_{xx} + \sigma_{yy}}{2}\right) + \left\{\left(\frac{\sigma_{xx} - \sigma_{yy}}{2}\right)^2 + \tau_{xy}^2\right\}^{1/2} \quad \ldots \quad (4b)$$

Fig.11 shows the rib pillars of the stope. Locations 1, 2, 3 and 4 (Fig.10) has the major and minor principal stresses are negative (-ve) and positive (+ve) respectively. It is clearly

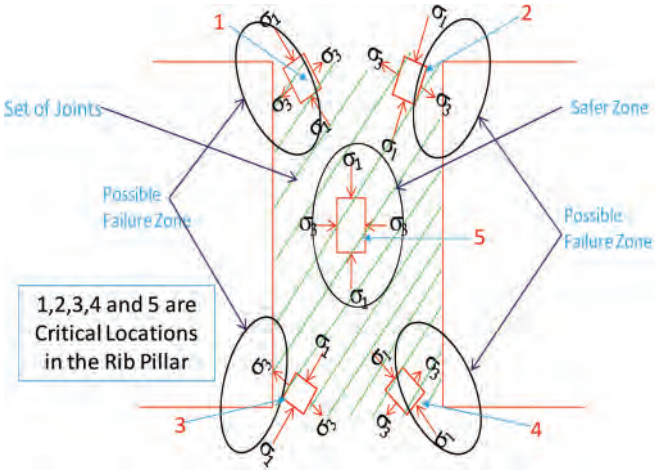

Fig.10 Set of joints and critical locations in the rib pillar

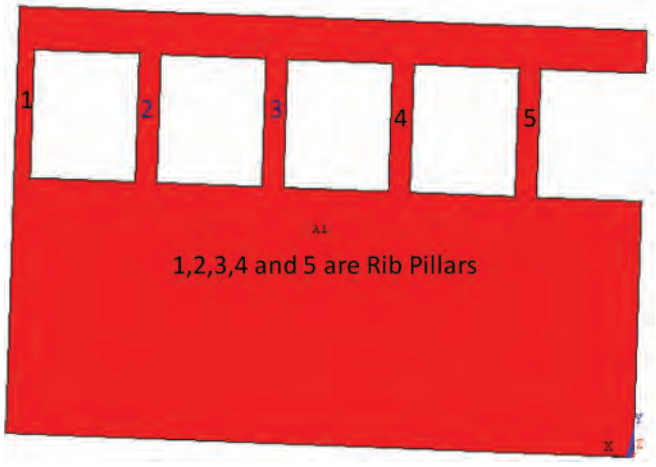

Fig.11 Rib pillars of the stope

seen that the shear and tensile stresses can occur in those locations and they may fail due to the shear and tensile stresses. Location 5 (Fig.10) has the major and minor principal stresses are negatives (-ve) and it is in compression. In order to analyze joint stick-slip behaviour, it is required to transform normal and shear stresses along the joint plane axis. Then Mohr-Coulomb criterion can be applied to check for onset of joint slip phenomenon.

According to Mohrs Coulomb theory:

$$\tau_j = c_j - \sigma_n \tan \phi_j \quad \ldots \quad (5a)$$

Failure may occur due to the joints if τ_j is greater than $c_j - s_n \tan f_j$ otherwise it will be safer. Stresses are transformed in the joint axes to perform the joint analysis (Fig.12) as mentioned below [7, 9].

$$\sigma_{Y''Y} = \left(\frac{\sigma_{xx}+\sigma_{yy}}{2}\right) - \left(\frac{\sigma_{xx}-\sigma_{yy}}{2}\right)\cos 2\theta - \tau_{xy}\sin 2\theta \quad \ldots (5b)$$

$$\tau_{X'Y} = -\left(\frac{\sigma_{xx}-\sigma_{yy}}{2}\right)\sin 2\theta + \tau_{xy}\cos 2\theta \quad \ldots \quad (5c)$$

where, $\sigma_{X'Y'} = \tau_j$, $\sigma_{Y'Y'} = \sigma_n$, ϕ_j is angle of internal friction of joint plane, $C_j - \sigma_n \tan(\Phi_j)$ is shear strength of joint plane, C_j is cohesion of joint plane, θ is dip angle of joint plane.

The joint analysis has been performed for all the locations of the rib pillars as listed in Table 3 and assumed angle of internal friction, dip angle and cohesions are 35^0, 65^0 and 3 MPa respectively. It is observed that locations 3 and 4 may fail and the other locations are safe [2].

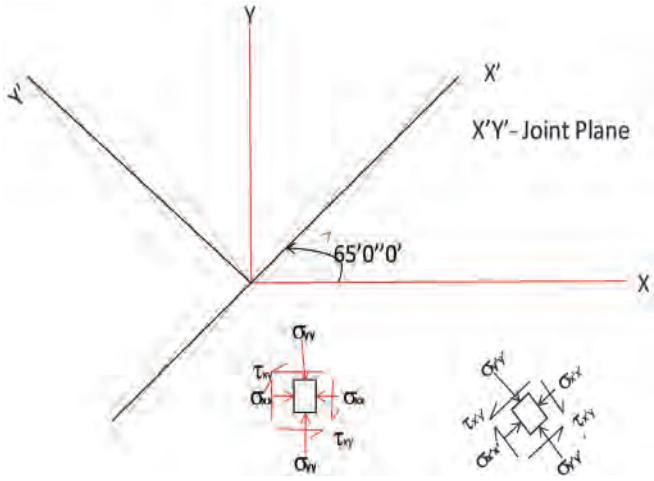

Fig.12 Joint plane in the rib pillar

Conclusions

1. Rock cores from various boreholes namely, No. 4, 5, 8, 11 and 13 of chromite orebody are tested. It is found that weathered and heavily jointed rocks exist up to 40 m below ground. Laboratory tests of uni-axial compressive and tensile strength suggest that the serpentenite rock is competent with UCS ranging from 82.34 to 229.55 MPa and tensile strength ranging between 3.62 to 29.96 MPa. The chromite rock is weathered at different locations and its UCS ranges between 33.46 to 193.98 MPa.
2. The maximum major principal stress of 31 MPa may occur in the rib pillars. The compressive major principal stress occurs at the crown pillars with a range between 3.43 and 13.8 MPa. A positive value of minor pricipal stress confirms the tensile stress in the rock mass and if this value exceeds the tensile strength of the rock mass, it can be assumed that tensile failure/yielding occurs. Tensile stress of 1 ~ 2 MPa develops at the roof of the stope (in crown pillar) and tensile stress of about 2.2 MPa has developed at the rib pillars.
3. From 2D finite element analysis, it is found that failure zone may occur in the rock mass surrounding the roof of stope area. To minimize this effect, fully grouted bolts will be required to support the roof and walls of cross-cuts. The length of bolt would be at least 2.4 m with a spacing of 1.2 m. The spacing can be reduced depending on the rock mass conditions.

Table 3: Condition of joints in different conditions

Location		σ_{XX} (MPa)	σ_{YY} (MPa)	σ_{XY} (MPa)	σ_n (MPa)	τ_j (MPa)	$Cj - \sigma_n \tan(\Phi j)$ (MPa)	Condition
Rib pillar 1	1	-6.92	-2.652	4.326	-9.471	1.15	9.63	Safe
	2	-5.792	-8.22	7.230	-12.000	5.58	11.24	Safe
	3	-6.390	-6.08	-5.424	-2.180	3.61	4.53	Fail
	4	-3.426	-13	-6.582	-0.022	0.72	3.02	Fail
	5	-0.03423	-1.908	-0.046	-0.333	0.69	3.23	Safe
Rib pillar 2	1	-1.36	-8.058	-1.074	-1.734	1.88	4.21	Safe
	2	-1.979	-8.81	1.382	-4.258	3.50	5.98	Safe
	3	-1.837	-10	1.103	-4.202	3.97	5.94	Safe
	4	0.172	-10	-0.370	-1.442	3.83	4.01	Safe
	5	-0.00033	-9.26	0.021	-1.670	3.56	4.17	Safe
Rib pillar 3	1	-1	-10	-0.846	-1.967	2.92	4.38	Safe
	2	-0.77	-9.852	1.110	-3.242	4.19	5.27	Safe
	3	-0.62	-12	1.456	-3.766	5.30	5.64	Safe
	4	-2.36	-12	-1.138	-3.121	2.77	5.19	Safe
	5	-0.00018	-11	-0.048	-1.893	4.11	4.33	Safe
Rib pillar 4	1	-1.032	-10	-0.873	-2.016	2.98	4.41	Safe
	2	-0.68	-9.59	1.014	-3.046	4.07	5.13	Safe
	3	-0.582	-12	1.340	-3.589	5.11	5.51	Safe
	4	-2.17	-12	-1.140	-2.995	2.91	5.10	Safe
	5	-0.00016	-11	-0.088	-1.867	4.09	4.31	Safe
Rib pillar 5	1	-1.725	-8.99	-1.446	-1.915	1.85	4.34	Safe
	2	-1.974	-7.66	1.227	-3.929	2.97	5.75	Safe
	3	-0.104	-10	0.304	-2.127	4.04	4.49	Safe
	4	-1.4	-11	-0.995	-2.353	3.08	4.65	Safe
	5	-0.00043	-9.507	-0.124	-1.604	3.56	4.12	Safe

4. From the joint analysis, it is found that the locations 3 and 4 of the rib pillar 1 may fail due to shear and tensile stress concentrations and all other locations of the rib pillar 1 will be in safe conditions. All the locations of the rib pillars 2, 3, 4 and 5 will be in safe condition.

References

1. Deb, D., Mukhopadhyay, S. K. and Suman, R. (2007): "Efficacy of numerical analysis on stability of stope applying three dimensional finite element method for a chromite orebody." *Journal of the Mining, Geological & Metallurgical Institute of India*. 2007; 10: 83-93.
2. Islavath, S. R. (2012): Stability analysis of vertical shaft, decline and stope pillars using numerical modelling techniques. M Tech thesis. IIT Kharagpur, India. 2012.
3. Islavath, S. R., Deb, D. and Bharti, S. (2015): "Design of lining for a mine shaft and decline using numerical modelling techniques." *ISRM (India) Journal*. 2015; 4(1):28-34.
4. Martin, C. D. and Maybee, W. G. (2000): "The strength of hard rock pillars." *International Journal of Rock Mechanics and Mining Sciences*. 2000; 1239-1246.
5. Agustawijaya, D. S. (2006): "The uniaxial compressive strength of soft rock." *International Journal of Rock Mechanics and Mining Sciences*. 2006; 241-246.
6. Bathe, K. G. (1995): Finite element procedure. Eglewood Cliffs, NJ: Prentice Hall. 1995.
7. Deb, D. (2011): Finite element method concepts and applications in geo mechanics. PHI Learning Pvt Limited, 2nd Edition, New Delhi, India. 2011; 259-305.
8. Gioda, G. and Swoboda, G. (1999): "Developments and applications of the numerical analysis of tunnels in continuous media." *International Journal for Numerical and Analytical Methods in Geomechanics*. 1999; 1-2.
9. Brady, B. H. G. and Brown, E. T. (2007): Rock mechanics for underground mining, third edition. Springer publication. 2007.